

FLOWTS: Time Series Generation via Rectified Flow

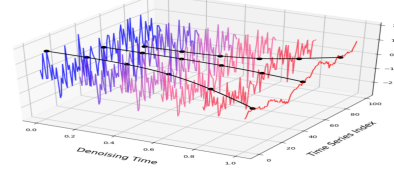
Yang Hu^{*1} Xiao Wang^{*2} Zezhen DING^{*3} Lirong Wu¹ Huatian Zhang⁴ Stan Z. Li¹ Sheng Wang²
Jiheng Zhang³ Ziyun Li^{†5} Tianlong Chen^{†6}

Abstract

Diffusion-based models have significant achievements in time series generation but suffer from *inefficient computation*: solving high-dimensional ODEs/SDEs via iterative numerical solvers demands hundreds to thousands of drift function evaluations per sample, incurring prohibitive costs. To resolve this, we propose FLOWTS, an ODE-based model that leverages rectified flow with *straight-line transport* in probability space. By learning geodesic paths between distributions, FLOWTS achieves computational efficiency through exact linear trajectory simulation, accelerating training and generation while improving performances. We further introduce an adaptive sampling strategy inspired by the exploration-exploitation trade-off, balancing noise adaptation and precision. Notably, FLOWTS enables seamless adaptation from unconditional to conditional generation without retraining, ensuring efficient real-world deployment. Also, to enhance generation authenticity, FLOWTS integrates trend and seasonality decomposition, attention registers (for global context aggregation), and Rotary Position Embedding (RoPE) (for position information). For unconditional setting, extensive experiments demonstrate that FLOWTS achieves state-of-the-art performance, with context FID scores of 0.019 and 0.011 on Stock and ETTh datasets (prev. best: 0.067, 0.061). For conditional setting, we have achieved superior performance in solar forecasting (MSE 213, prev. best: 375) and MuJoCo imputation tasks (MSE 7e-5, prev. best 2.7e-4). The code is available at <https://github.com/UNITES-Lab/FlowTS>.

^{*}Equal contribution [†]Co-Corresponding ¹Westlake University ²University of Washington ³The Hong Kong University of Science and Technology ⁴University of Science and Technology of China ⁵KTH Royal Institute of Technology ⁶Department of Computer Science, University of North Carolina at Chapel Hill. Correspondence to: Tianlong Chen <tianlong@cs.unc.edu>, Ziyun Li <liziyn2014@gmail.com>.

$$DDPM: Z_t = \sqrt{\alpha_t}Z_1 + \sqrt{1 - \alpha_t}Z_0$$



$$Rectified\ Flow: Z_t = tZ_1 + (1 - t)Z_0$$

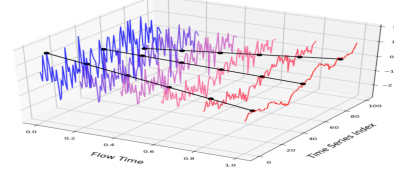


Figure 1: **Process evolution comparison** The evolution processes from initial state $Z_0 \sim \pi_0$ (blue) to final state $Z_1 \sim \pi_1$ (red) are visualized for both models. The intermediate states (purple) illustrate the continuous evolution between the two endpoints. Rectified Flow exhibits a linear transformation path, while DDPM demonstrates a curved trajectory from Z_0 to Z_1 .

1. Introduction

Recent years have seen significant advancements in time series generation, including VAE-based approaches (De-sai et al., 2021; Xu et al., 2020), GAN-based methods, and diffusion-based techniques (Kong et al., 2021; Tashiro et al., 2021). Among these, diffusion-based methods have demonstrated leading performance by explicitly modeling the iterative denoising process, enabling high-quality reconstructions. Despite these strengths, a critical limitation persists: *inefficient computation*. Generating a single sample requires solving high-dimensional Ordinary/Stochastic Differential Equations (ODEs/SDEs) through iterative numerical solvers, necessitating hundreds to thousands of evaluations of the parameterized drift function, a prohibitive cost for real-world deployment. Furthermore, optimizing these models demands extensive hyperparameter searches in complex design spaces (Karras et al., 2022), complicating their adoption even in resource-rich settings.

To address this limitation, we propose FLOWTS, an ODE-based generative model designed for highly efficient time

series generation. Unlike iterative denoising diffusion methods, FLOWTS learns to transport the data distribution π_0 to the target π_1 via straight-line paths in the probability space. The process evolution comparison is demonstrated in Figure 1. By bridging the gap between one-step and continuous-time models, FLOWTS unifies two key advantages: *i*) theoretical optimality through transport-cost-minimizing geodesics; *ii*) computational efficiency via exact simulation along straight trajectories, eliminating iterative steps. This design accelerates both training and generation while stabilizing the training process by reducing numerical error. Furthermore, by employing straight-line paths and an unconstrained least-squares procedure for its rectified flow (Liu et al., 2022), FLOWTS avoids the instability issues common to GANs. We also propose a simple yet highly effective adaptive sampling strategy, inspired by the exploration-exploitation trade-off (Sutton & Barto, 2018), which optimally balances an early focus on accommodating higher noise levels with a subsequent shift toward denser and more precise sampling. Notably, FLOWTS’s novel inference mechanism allows a model trained in unconditional settings to seamlessly adapt to conditional tasks without retraining.

Another key challenge for time series generation is to ensure its authenticity. Following previous practice in diffusion models (Yuan & Qiao, 2024), we also incorporate trend and seasonality components to explicitly capture periodic and long-term patterns. However, such explicit decomposition often neglects unobserved global dependencies (e.g., latent interactions). To bridge this gap, we exploit attention register tokens (Darcet et al., 2023) to aggregate global context across series and Rotary Position Embedding (RoPE) (Su et al., 2024) to encode positional information via rotation matrices. The extensive experiments validated FLOWTS can effectively capture both local and global dependencies through these designs, significantly enhancing the authenticity of generated time series.

In summary, this paper has the following contributions:

- We introduce FLOWTS, a pioneering approach that utilizes rectified flow with ODE-based straight-line transport for time series generation. This design achieves highly efficient generation, and an adaptive sampling strategy further balances exploration and exploitation for improved sample quality.
- We explicitly model global information and positional structure using attention register and RoPE, enhancing the authenticity of generated time series.
- FLOWTS achieves state-of-the-art performance, with context FID scores of 0.019 and 0.011 on Stock and ETTh datasets (prev. best: 0.067, 0.061). In solar forecasting, it lowers MSE to 213, a 43.2% improvement over the previous best of 375.

2. Related Work

2.1. Time Series Generation

VAE & GAN-based Models VAE (Desai et al., 2021) and GAN (Goodfellow et al., 2014). TimeVAE (Desai et al., 2021) introduces a hierarchical latent structure to better capture temporal dependencies, while TimeGAN (Yoon et al., 2019) combines adversarial training with supervised learning to preserve both temporal dynamics and feature distributions. CotGAN (Xu et al., 2020) further improves GAN-based generation by incorporating optimal transport theory to stabilize training.

Diffusion-based Models Diffusion models, particularly DDPMs (Ho et al., 2020), emerge as a powerful generative paradigm, offering superior perceptual quality over GANs while avoiding training instability and mode collapse. In time series, Diffwave (Kong et al., 2020) pioneers the application of diffusion models to time-varying data through audio synthesis. For conditional generation, TimeGrad (Rasul et al., 2021) employs autoregressive prediction with RNN guidance, while CSDI (Tashiro et al., 2021) and SSSD (Alcaraz & Strodthoff, 2022a) extend the framework to handle irregular time series and missing data imputation using self-supervised masking strategies. For unconditional generation, TimeDiff (Shen & Kwok, 2023) adopts a non-autoregressive approach to mitigate boundary disharmony, while (Lim et al., 2023) leverages RNNs within Score-based Generative Models (SGMs) (Song et al., 2021) for regular series generation. More recently, TSDiff (Kollovieh et al., 2024) introduces self-guided generation with structured state space models, while Diffusion-TS (Yuan & Qiao, 2024) enhances temporal modeling with specialized architectures.

2.2. Flow Matching

Flow matching (Liu et al., 2022; Lipman et al., 2022) has emerged as a promising alternative to diffusion models. While diffusion models learn to gradually denoise data through a stochastic process, flow matching directly learns the velocity field of a continuous-time transformation, providing deterministic paths with minimal steps. Flow matching achieves remarkable results across various domains including video generation (Kuaishou Technology, 2024), image generation (Esser et al., 2024), point cloud generation (Wu et al., 2023), protein design (Campbell et al., 2024; Jing et al., 2024), human motion synthesis (Hu et al., 2023), and speech synthesis (Mehta et al., 2024). Recent work CFM-TS (Tamir et al., 2024) shows promising results in applying flow matching to Neural ODEs (Chen et al., 2018) for time series modeling through conditional probability paths, though its application to time series generation remains unexplored.

3. FLOWTS

In this section, we first define the problem statement, outlining the objectives. Next, we present the core components of FLOWTS, including Rectified Flow-based framework, adaptive sampling strategy, and model architecture.

3.1. Problem Statement

Unconditional Generation Unconditional time series generation aims to produce sequential data without partially observed data, where the model learns temporal patterns from a training set and generates new sequences following the same distribution. Let $X_{1:\ell} = (x_1, \dots, x_\ell) \in \mathbb{R}^{\ell \times d}$ denote a time series of length ℓ , where d is the number of observed dimensions. The problem is defined as follows:

$$\begin{aligned} \text{Input: } & Z_0 \sim \pi_0; \\ & \text{where } Z_0 \in \mathbb{R}^{\ell \times d}, \pi_0 = \mathcal{N}(0, I). \\ \text{Output: } & \hat{X}_{1:\ell} = G(Z_0) \in \mathbb{R}^{\ell \times d}; \\ & G \text{ maps } Z_0 \text{ to the target distribution.} \end{aligned} \quad (1)$$

We define Z_0 as the initial state, and the generative model G can be implemented using GANs (Yoon et al., 2019), VAEs (Desai et al., 2021), or diffusion models (Tashiro et al., 2021; Yuan & Qiao, 2024), which effectively capture complex temporal dependencies. During training, G is optimized to minimize the discrepancy between the generated $\hat{X}_{1:\ell}$ and the target $X_{1:\ell}$, ensuring high fidelity and diversity in the generated sequences.

Conditional Generation Conditional time series generation produces sequences by leveraging partially observed data y as context. The generated sequence includes both observed and predicted segments. Formally:

$$\begin{aligned} \text{Input: } & Z_0 \sim \pi_0, \quad y \in \mathbb{R}^{m \times d}; \\ & y \text{ is the observed time series with length } m. \\ \text{Output: } & \hat{X}_{1:\ell} = G(Z_0; y) \in \mathbb{R}^{\ell \times d}; \\ & G \text{ maps } Z_0 \text{ to the target distribution given } y. \end{aligned} \quad (2)$$

Conditional time series generation can be divided into two main tasks: *i) Forecasting*: G predicts future values from past observations, given $y = (x_1, x_2, \dots, x_m)$ represents observed values up to time m , and the goal is to predict values for $m+1, m+2, \dots, \ell$. *ii) Imputation*: G fills unobserved series, where y represents m observed series within the range 1 to ℓ . The key difference between forecasting and imputation lies in the position of known observations.

3.2. Rectified Flow for Time Series Generation

To tackle the efficiency challenges in time series generation, we propose FLOWTS, leveraging rectified flow as the generative model G . Rectified flow (Liu et al., 2022) learns

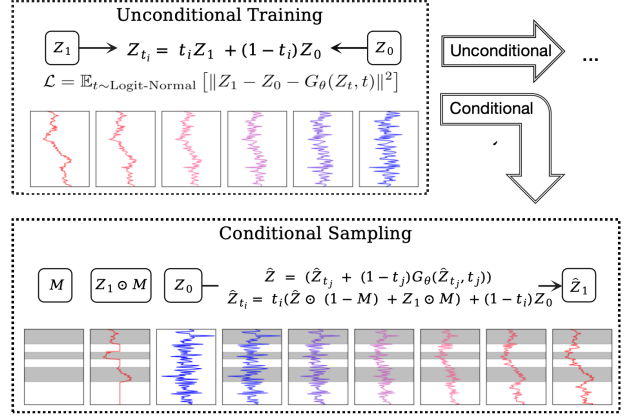


Figure 2: **FLOWTS pipeline.** FLOWTS is trained to learn an ODE to transport samples from Z_0 to Z_1 via a linear path. After training, through adaptive sampling, FLOWTS can be applied to both unconditional and conditional generation. The details of sampling are included in Algorithm 1 and 2, respectively.

an ODE to transport samples between two distributions, π_0 and π_1 . Therefore, the above problem can be formulated as learning a transport map $G : \mathbb{R}^{\ell \times d} \rightarrow \mathbb{R}^{\ell \times d}$, such that $Z_1 := G(Z_0)$ follows the target distribution π_1 when $Z_0 \sim \pi_0$. By learning G , samples from π_0 are transformed to match the target distribution π_1 , enabling both unconditional and conditional time series generation.

The rectified flow induced from (Z_0, Z_1) is defined as an ODE over time $t \in [0, 1]$:

$$\frac{dZ_t}{dt} = v(Z_t, t), \quad \text{where } t \in [0, 1], Z_t \in \mathbb{R}^{\ell \times d}, \quad (3)$$

$Z_t \in \mathbb{R}^{\ell \times d}$ represents the state at time t , $v : \mathbb{R}^{\ell \times d} \rightarrow \mathbb{R}^{\ell \times d}$ is the drift function designed to drive the flow along the direction of the linear path $(Z_1 - Z_0)$, ensuring the transformation follows this trajectory as closely as possible. This can be achieved by solving a least squares regression problem:

$$\min_v \int_0^1 \mathbb{E} [\|Z_1 - Z_0 - v(Z_t, t)\|^2] dt, \quad (4)$$

where Z_t is a linear interpolation between Z_0 and Z_1 , $Z_t = tZ_1 + (1-t)Z_0$, and v is expected to learn with the neural network G . Therefore, model G can be optimized by predicting the direction vector between $(Z_1 - Z_0)$ via the following loss function:

$$\mathcal{L} = \mathbb{E}_{t \sim \text{Logit-Normal}} [\|(Z_1 - Z_0) - G(Z_t, t)\|^2], \quad (5)$$

where G is the model used in FLOWTS to learn the drift force v . For each sample, t is randomly drawn from a Logit-Normal distribution (Esser et al., 2024), while Z_1 is

sampled from the target time series distribution π_1 , and Z_0 is sampled from the standard normal distribution π_0 .

The overall framework is illustrated in Fig. 2. The unconditional time series generation model G is trained using the loss in Eq. 5, where it takes Z_t and t as inputs to predict the drift force v between Z_0 and Z_1 . Once trained, the unconditional model can be directly applied to conditional generation tasks without requiring task-specific training for a separate conditional model. Instead, it can be achieved by a simple adaptive sampling, illustrated in Section 3.3.

Algorithm 1 FlowTS unconditional generation

Require: Sampling iterations N , adaptive parameter k , trained flow matching model G_θ

- 1: $\hat{Z}_0 \sim \mathcal{N}(0, \mathbf{I})$ ▷Sample initial noise
- 2: $t_0 = 0$ ▷Initialize time step
- 3: **for** $i = 0$ to $N - 1$ **do**
- 4: $t_{i+1} = ((i + 1)/N)^k$ ▷Get next adaptive time step
- 5: $\hat{v}_{t_i} = G_\theta(\hat{Z}_{t_i}, t_i)$ ▷Get velocity from model
- 6: $\hat{Z}_{t_{i+1}} = \hat{Z}_{t_i} + (t_{i+1} - t_i)\hat{v}_{t_i}$ ▷One Euler step
- 7: **end for**
- 8: **return** \hat{Z}_1

3.3. Adaptive Sampling

The exploration-exploitation trade-off balances discovering new strategies and leveraging known ones, a key concept in decision-making under uncertainty (Sutton & Barto, 2018; Lattimore & Szepesvári, 2020; Jin et al., 2018; Agarwal et al., 2021). Inspired by this, we introduce adaptive sampling by using a scaling factor t^k , where $k \in (0, 1]$ ($k = 1$ represents uniform sampling). Early in the process, t^k promotes exploration by encouraging the model to estimate higher noise levels, while in later stages, it focuses on exploitation through denser, smaller sampling steps. Furthermore, we observe that as the number of sampling iterations increases, the optimal k decreases. Detailed experiments on the impact of k are provided in Section 4.4.

For unconditional sampling, we utilize ODE sampling along a straightened trajectory. This method reduces the number of sampling steps, enabling faster inference while maintaining performance, as detailed in Algorithm 1. For conditional sampling, inspired by (Song et al., 2020), we used the observed segment as context to refine the sampling process. As described in Algorithm 2, the conditional generation includes two main novel designs compared to unconditional setting. First, it utilized the observed Z_1 to refine the \hat{Z}_1 estimation (line 5) at every iteration. Then, it will interpolate the \hat{Z}_t at timestep t given refined \hat{Z}_1 (line 6). After that, it will be same as the unconditional generation to estimate the \hat{Z}_{t+1} at next timestep $t + 1$. Therefore, our framework enables seamless adaptation from unconditional to conditional

generation without retraining.

Algorithm 2 FlowTS conditional generation

Require: Target time series Z_1 , observation mask \mathbf{M} , sampling iterations N , adaptive parameter k , trained flow matching model G_θ

- 1: $\hat{Z}_1 \sim \mathcal{N}(0, \mathbf{I})$ ▷Initialize with random noise
- 2: **for** $i = 0$ to $N - 1$ **do**
- 3: $t_i = (i/N)^k$ ▷Compute adaptive time step
- 4: $Z_0 \sim \mathcal{N}(0, \mathbf{I})$ ▷Sample noise
- 5: $\hat{Z}_1 = \hat{Z}_1 \odot (1 - \mathbf{M}) + Z_1 \odot \mathbf{M}$ ▷Replace with observed values
- 6: $\hat{Z}_{t_i} = t_i \hat{Z}_1 + (1 - t_i) Z_0$ ▷Interpolate
- 7: $\hat{v}_{t_i} = G_\theta(\hat{Z}_{t_i}, t_i)$ ▷Flow matching step
- 8: $\hat{Z}_1 = \hat{Z}_{t_i} + (1 - t_i)\hat{v}_{t_i}$ ▷One Euler step
- 9: **end for**
- 10: **return** \hat{Z}_1

3.4. Model Architecture

Overview As shown in Figure 3, FLOWTS is based on the encoder-decoder Transformer (Vaswani, 2017), with blue components as the standard structure and green highlighting novel additions. Attention register (Darcet et al., 2023) enhances the model’s memory capability and information transmission efficiency, enabling efficient capture of global dependencies. The integration of Rotary Position Embedding (RoPE) (Su et al., 2024) provides precise relative positional encoding, enhancing the model’s ability to represent temporal relationships effectively. Inspired by (Yuan & Qiao, 2024), our model incorporates trend synthetic layers and fourier synthetic layers to capture the trend and periodic patterns. This design improves interpretability by decomposing the prediction target into residual, mean, trend, and seasonality components.

Attention Register As shown in Figure 3, attention registers are learnable tokens that serve as dedicated computational units, distinct from the main sequence tokens (Darcet et al., 2023). As persistent memory, these registers capture and maintain global patterns, allowing sequence tokens to focus on local temporal dependencies. This mechanism has proven effective in vision (Darcet et al., 2023) and language models (Xiao et al., 2023). Thus we integrate learnable register tokens into our architecture to capture global information.

Rotary Position Embedding (RoPE) RoPE (Su et al., 2024) is a position encoding mechanism that enhances the standard Transformer architecture by encoding positional information through rotation matrices. We also incorporate RoPE into our time series generation framework for two key advantages: *i*) its natural decay property, which aligns with temporal dependencies in time series data, and *ii*) its

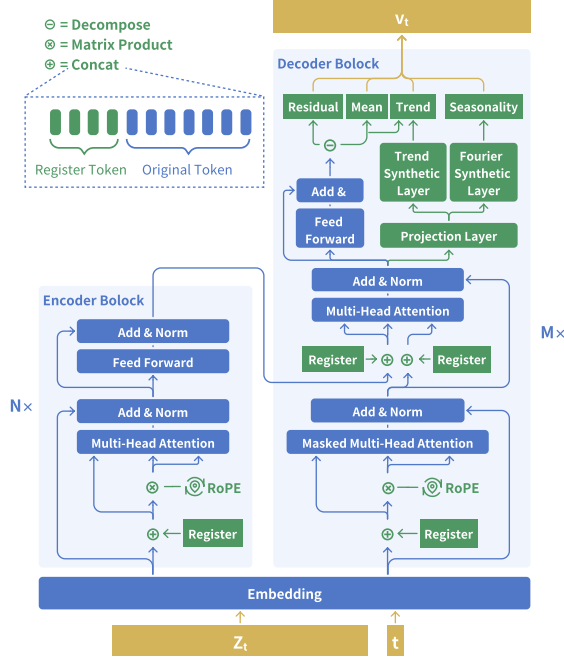


Figure 3: The FLOWTS model builds on the standard Transformer architecture. The blue components represent the basic encoder-decoder structure, while the green components highlight novel additions, including attention registers, RoPE, Trend and Fourier Synthetic Layers. The model processes input Z_t and timestep t through N encoder and M decoder blocks to produce the drift force v_t at time t .

flexibility in handling varying sequence lengths.

4. Experiments

4.1. Experiment Setup

Datasets Our evaluation employs six diverse datasets: the three real-world datasets include *Stocks*¹ for measuring daily stock price data, *ETTh*² (Zhou et al., 2021) for interval electricity transformer data, and *Energy*³ for UCI appliance energy prediction. The three simulation data sets include *fMRI*⁴ for simulated blood-oxygen-level-dependent time series, *Sines*⁵ (Yoon et al., 2019) generated from different frequencies, amplitudes, and phases, and *Mujoco*⁶ from multivariate simulation of physics. These datasets capture diverse time series characteristics, including periodicity, dimensionality, and feature correlation, ensuring a compre-

¹finance.yahoo.com/quote/GOOG/history?p=GOOG

²github.com/zhouhaoyi/ETDataset

³archive.ics.uci.edu/ml/datasets/Appliances+energy+prediction

⁴fmrilab.ox.ac.uk/datasets/netsim/

⁵github.com/jsyoon0823/TimeGAN

⁶github.com/google-deepmind/dm.control

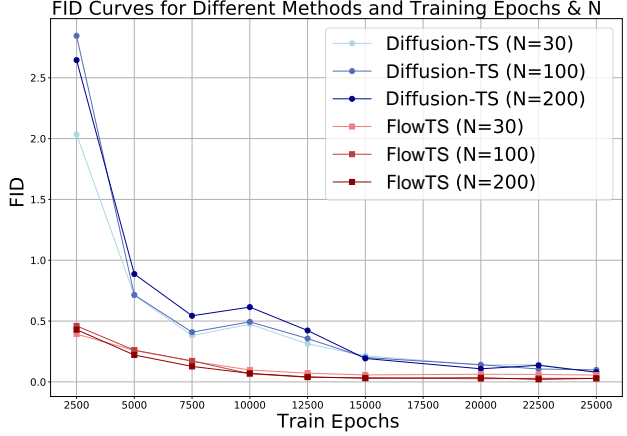


Figure 4: FID curves of FLOWTS and Diffusion-TS on Energy dataset across training epochs (2,500–25,000) and sampling steps. FLOWTS demonstrates superior efficiency, achieving lower FID scores with fewer training and sampling epochs.

hensive evaluation of our approach.

Metrics Following the practices of time series generation (Yuan & Qiao, 2024), we evaluate our method using four metrics: 1) **Discriminative Score** (Yoon et al., 2019), which measures distributional similarity between real and synthetic data using a 2-layer LSTM classifier; lower classification error indicates higher-quality synthetic data. 2) **Predictive Score** (Yoon et al., 2019), which assesses the utility of synthetic data for prediction tasks by training a 2-layer LSTM on synthetic data and testing on real data, with performance measured by mean absolute error (MAE). 3) **Context-FID** (Jeha et al., 2022), which quantifies quality by comparing contextual representations, capturing both distributional similarity and temporal dependencies. 4) **Correlational Score** (Liao et al., 2020), which evaluates the preservation of temporal dependencies by comparing cross-correlation matrices, where lower errors indicate better structural fidelity. These metrics provide a comprehensive evaluation of the quality, utility, and temporal consistency of synthetic time series data.

Baselines & Implementation Details We evaluate our method for unconditional time series generation by comparing with six baseline models: Diffusion-TS (Yuan & Qiao, 2024), TimeGAN (Yoon et al., 2019), TimeVAE (Desai et al., 2021), Diffwave (Kong et al., 2020) and CotGAN (Xu et al., 2020). For conditional tasks, we also compare our method against CSDI (Tashiro et al., 2021) and SSSD (Alcaraz & Strodthoff, 2022a). For a fair comparison, we closely follow the Diffusion-TS experimental setup, using the same hyperparameters, including batch size, attention heads, learning rate (AdamW), training iterations, etc. Specifically, for 24-length, we use 4 attention

Table 1: Unconditional time series generation benchmark with 24-length

Metric	Methods	Sines	Stocks	ETTh	MuJoCo	Energy	fMRI
Discriminative (Lower Better)	FLOWTS	0.005±.005	0.019±.013	0.011±.015	0.005±.005	0.053±.010	0.106±.018
	Diffusion-TS	0.006±.007	0.067±.015	0.061±.009	0.008±.002	0.122±.003	0.167±.023
	TimeGAN	0.011±.008	0.102±.021	0.114±.055	0.238±.068	0.236±.012	0.484±.042
	TimeVAE	0.041±.044	0.145±.120	0.209±.058	0.230±.102	0.499±.000	0.476±.044
	Diffwave	0.017±.008	0.232±.061	0.190±.008	0.203±.096	0.493±.004	0.402±.029
	DiffTime	0.013±.006	0.097±.016	0.100±.007	0.154±.045	0.445±.004	0.245±.051
	Cot-GAN	0.254±.137	0.230±.016	0.325±.099	0.426±.022	0.498±.002	0.492±.018
Predictive (Lower Better)	FLOWTS	0.092±.000	0.036±.000	0.118±.005	0.008±.001	0.250±.000	0.099±.000
	Diffusion-TS	0.093±.000	0.036±.000	0.119±.002	0.007±.000	0.250±.000	0.099±.000
	TimeGAN	0.093±.019	0.038±.001	0.124±.001	0.025±.003	0.273±.004	0.126±.002
	TimeVAE	0.093±.000	0.039±.000	0.126±.004	0.012±.002	0.292±.000	0.113±.003
	Diffwave	0.093±.000	0.047±.000	0.130±.001	0.013±.000	0.251±.000	0.101±.000
	DiffTime	0.093±.000	0.038±.001	0.121±.004	0.010±.001	0.252±.000	0.100±.000
	Cot-GAN	0.100±.000	0.047±.001	0.129±.000	0.068±.009	0.259±.000	0.185±.003
	Original	0.094±.001	0.036±.001	0.121±.005	0.007±.001	0.250±.003	0.090±.001
Context-FID (Lower Better)	FLOWTS	0.002±.000	0.015±.003	0.024±.001	0.009±.000	0.031±.004	0.128±.009
	Diffusion-TS	0.006±.000	0.147±.025	0.116±.010	0.013±.001	0.089±.024	0.105±.006
	TimeGAN	0.101±.014	0.103±.013	0.300±.013	0.563±.052	0.767±.103	1.292±.218
	TimeVAE	0.307±.060	0.215±.035	0.805±.186	0.251±.015	1.631±.142	14.449±.969
	Diffwave	0.014±.002	0.232±.032	0.873±.061	0.393±.041	1.031±.131	0.244±.018
	DiffTime	0.006±.001	0.236±.074	0.299±.044	0.188±.028	0.279±.045	0.340±.015
	Cot-GAN	1.337±.068	0.408±.086	0.980±.071	1.094±.079	1.039±.028	7.813±.550
Correlational (Lower Better)	FLOWTS	0.015±.006	0.012±.011	0.022±.010	0.183±.051	0.650±.201	0.938±.039
	Diffusion-TS	0.015±.004	0.004±.001	0.049±.008	0.193±.027	0.856±.147	1.411±.042
	TimeGAN	0.045±.010	0.063±.005	0.210±.006	0.886±.039	4.010±.104	23.502±.039
	TimeVAE	0.131±.010	0.095±.008	0.111±.020	0.388±.041	1.688±.226	17.296±.526
	Diffwave	0.022±.005	0.030±.020	0.175±.006	0.579±.018	5.001±.154	3.927±.049
	DiffTime	0.017±.004	0.006±.002	0.067±.005	0.218±.031	1.158±.095	1.501±.048
	Cot-GAN	0.049±.010	0.087±.004	0.249±.009	1.042±.007	3.164±.061	26.824±.449

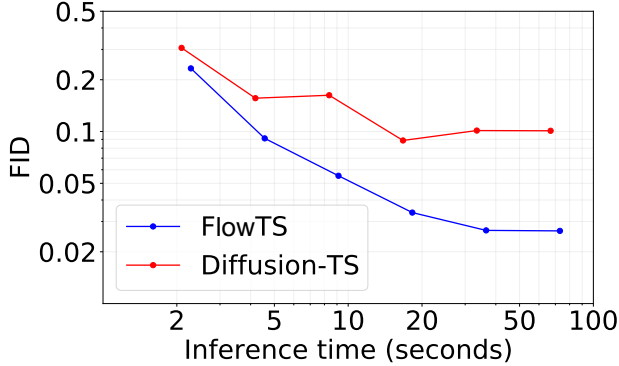


Figure 5: Context-FID scores with different sampling iterations (1, 2, 4, 8, 16, 32) on Energy, measured against cumulative sampling time. FLOWTS outperforms Diffusion-TS in both accuracy and sampling speed.

register tokens with RoPE set to a frequency of 50k. For 256-length, we increase the attention registers to 128 while keeping the RoPE frequency unchanged.

4.2. Higher Efficiency

Training Efficiency To evaluate training efficiency, we benchmarked FLOWTS and Diffusion-TS across multiple training iterations on the *Energy* dataset. As shown in Figure 4, FLOWTS consistently outperforms Diffusion-TS in achieving superior FID scores, with training itera-

tions ranging from 2,500 to 25,000. Remarkably, FLOWTS achieves superior performance with only 30 sampling iterations ($N = 30$) after just 2,500 training iterations, whereas Diffusion-TS fails to reach the same level of efficiency even with 200 inference steps ($N = 200$) after 10,000 training iterations.

Inference Efficiency To assess inference efficiency, we measure the sampling time (seconds) on the *Energy* dataset with varying sampling steps (1, 2, 4, 8, 16, 32) for Diffusion-TS and FLOWTS. As shown in Figure 5, FLOWTS outperforms Diffusion-TS in both accuracy and sampling speed, demonstrating its efficiency in time series generation.

4.3. Better Performance

Unconditional Sampling As shown in Table 1, FLOWTS demonstrates significantly superior performance across all evaluation metrics compared to all baselines on short-term 24-length time series. For the Discriminative Score, FLOWTS reduces error by up to 50% compared to Diffusion-TS (e.g., 0.005 vs. 0.006 on Sines). On the Predictive Score, FLOWTS matches or slightly improves upon Diffusion-TS (e.g., 0.036 vs. 0.036 on Stocks). For Context-FID, FLOWTS achieves up to 33% lower scores (e.g., 0.009 vs. 0.013 on MuJoCo), while for the Correlational Score, it provides up to 15% better temporal correlation preservation (e.g., 0.938 vs. 1.411 on fMRI). Also, FLOWTS achieves superior performance on long-term time series generation across all metrics on the ETTh dataset. For Discrimina-

Table 2: Benchmark of Unconditional Long-term Time Series Generation on ETTh Datasets

Metric	Length	FLOWTS	Diffusion-TS	TimeGAN	TimeVAE	Diffwave	DiffTime	Cot-GAN
Discriminative (Lower Better)	64	0.010 ± 0.004	0.106 ± 0.048	0.227 ± 0.078	0.171 ± 0.142	0.254 ± 0.074	0.150 ± 0.003	0.296 ± 0.348
	128	0.040 ± 0.012	0.144 ± 0.060	0.188 ± 0.074	0.154 ± 0.087	0.274 ± 0.047	0.176 ± 0.015	0.451 ± 0.080
	256	0.081 ± 0.022	0.060 ± 0.030	0.444 ± 0.056	0.178 ± 0.076	0.304 ± 0.068	0.243 ± 0.005	0.461 ± 0.010
Predictive (Lower Better)	64	0.115 ± 0.005	0.116 ± 0.000	0.132 ± 0.008	0.118 ± 0.004	0.133 ± 0.008	0.118 ± 0.004	0.135 ± 0.003
	128	0.104 ± 0.013	0.110 ± 0.003	0.153 ± 0.014	0.113 ± 0.005	0.129 ± 0.003	0.120 ± 0.008	0.126 ± 0.001
	256	0.107 ± 0.005	0.109 ± 0.013	0.220 ± 0.008	0.110 ± 0.027	0.132 ± 0.001	0.118 ± 0.003	0.129 ± 0.000
Context-FID (Lower Better)	64	0.039 ± 0.003	0.631 ± 0.058	1.130 ± 0.102	0.827 ± 0.146	1.543 ± 0.153	1.279 ± 0.083	3.008 ± 0.277
	128	0.128 ± 0.007	0.787 ± 0.062	1.553 ± 0.169	1.062 ± 0.134	2.354 ± 0.170	2.554 ± 0.318	2.639 ± 0.427
	256	0.302 ± 0.018	0.423 ± 0.038	5.872 ± 0.208	0.826 ± 0.093	2.899 ± 0.289	3.524 ± 0.830	4.075 ± 0.894
Correlational (Lower Better)	64	0.027 ± 0.015	0.082 ± 0.005	0.483 ± 0.019	0.067 ± 0.006	0.186 ± 0.008	0.094 ± 0.010	0.271 ± 0.007
	128	0.030 ± 0.011	0.088 ± 0.005	0.188 ± 0.006	0.054 ± 0.007	0.203 ± 0.006	0.113 ± 0.012	0.176 ± 0.006
	256	0.025 ± 0.008	0.064 ± 0.007	0.522 ± 0.013	0.046 ± 0.007	0.199 ± 0.003	0.135 ± 0.006	0.222 ± 0.010

tive Score, it improves by up to 83% over the second-best method (e.g., 0.010 vs. 0.060 for length 64). For Predictive Score, it consistently outperforms, with up to 6% better results (e.g., 0.104 vs. 0.110 for length 128). On Context-FID, FLOWTS achieves scores up to 88% lower (e.g., 0.039 vs. 0.423 for length 64), and for Correlational Score, it preserves temporal structure with up to 61% improvement (e.g., 0.025 vs. 0.064 for length 256). These results highlight FLOWTS as the most effective method for both short term and long-term time series generation.

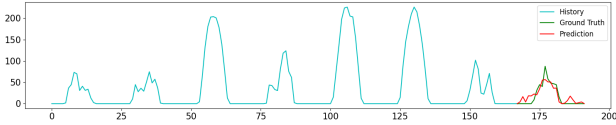


Figure 6: An example of solar forecasting results.

Conditional Sampling After validating FLOWTS on unconditional time series generation, we further assessed its generalizability for conditional time series generation. Without retraining the model, we utilized a specialized inference algorithm (Algorithm 2) to incorporate observed information during inference. As outlined in Section 3.1, conditional time series generation involves two key tasks: forecasting and imputation. To demonstrate the effectiveness of FLOWTS, we benchmarked it on the *Solar* and *Mujoco* datasets, following the practices in (Alcaraz & Strodtthoff, 2022b) and (Tashiro et al., 2021).

(i) **Forecasting:** Table 3 summarizes the forecasting performance on the *Solar* dataset. With a sequence length of 168, FLOWTS achieved a MSE of 213 for the next 24 time points, significantly outperforming Diffusion-TS (375). This demonstrates the superior prediction accuracy and sequence alignment of FLOWTS. Figure 6 further illustrates the forecasting results, showing how FLOWTS effectively captures the incoming peak in the future time series.

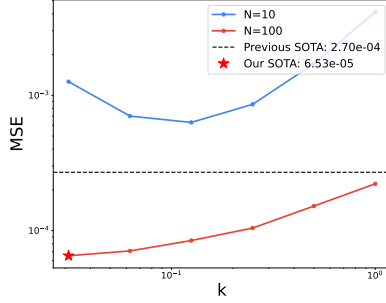
(ii) **Imputation:** We further evaluated FLOWTS on the imputation task using the MuJoCo dataset (Table 3), following the setup in (Alcaraz & Strodtthoff, 2022a). Despite most competing methods being tailored for conditional time series generation, FLOWTS consistently outperformed them under varying missing data ratios. Notably, for a 70% missing rate, it achieved a Mean Squared Error (MSE) of 0.00007, a 74.1% reduction compared to Diffusion-TS (0.00027), highlighting its superior imputation performance.

 Table 3: Time series forecasting on Solar and imputation on Mujoco. MSE results of Mujoco are in the order of $1e-3$.

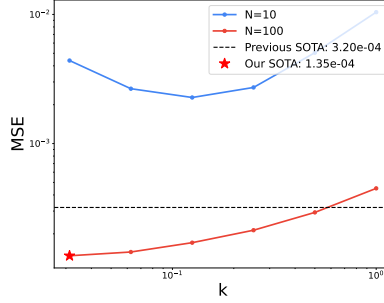
Model	Solar Forecasting	Mujoco Imputation	
	168 → 24	Missing(70 %)	Missing(80 %)
GP-copula	9.8e2	—	—
TransMAF	9.30e2	—	—
TLAE	6.8e2	—	—
RNN GRU-D	—	11.34	14.21
ODE-RNN	—	9.86	12.09
NeuralCDE	—	8.35	10.71
Latent-ODE	—	3.00	2.95
NAOMI	—	1.46	2.32
NRTSI	—	0.63	1.22
CSDI	9.0e2	0.24	0.61
SSSD	5.03e2	0.59	1.00
Diffusion-TS	3.75e2	0.27	0.32
FLOWTS	2.13e2	0.07	0.14

4.4. Further Experiments

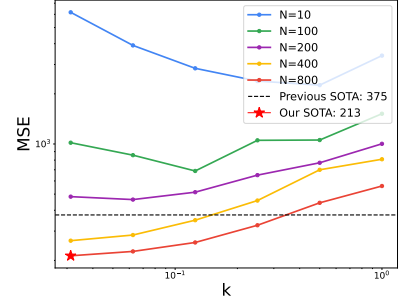
Ablation Study Table 4 shows that using both RoPE (frequency 50k) and attention registers (128 tokens) yields the lowest Context-FID score (0.1981 on ETTh, 0.1173 on Energy). Removing either component degrades performance: without both, FID scores rise sharply (0.9053 on ETTh, 0.3489 on Energy), while adding only RoPE offers partial improvement (0.2053 on ETTh, 0.3367 on Energy). This highlights the complementary benefits of positional encod-



(a) MSE with changing N and k on Mujoco dataset imputation tasks, with missing ratio 0.7



(b) MSE with changing N and k on Mujoco dataset imputation tasks, with missing ratio 0.8



(c) MSE with changing N and k on solar dataset forecasting tasks

Figure 7: Conditional generation with different k

ing and global context tokens.

Table 4: Ablation study of FID (lower is better) on ETTh and Energy, showing that combining RoPE (frequency 50k) and attention registers (128 tokens) achieves the best scores. Base model represents the model without RoPE and Register.

Configuration	ETTh	Energy
Base model	0.9053 ± 0.1611	0.3489 ± 0.0586
+RoPE	0.2053 ± 0.0191	0.3367 ± 0.0352
+RoPE +Register	0.1981 ± 0.0073	0.1173 ± 0.0134

k -selection In Fig. 7, we compare different values of $k \in (0, 1]$ for generation under varying numbers of sampling iterations N_s . We evaluate the imputation task on Mujoco and the forecasting task on Solar with missing ratios of 0.7 and 0.8. First, we demonstrate that adaptive sampling consistently achieves superior results across all settings. Second, we observe that as k decreases, the MSE loss also decreases, indicating more stable inference. This suggests that a smaller k can lead to better performance.

Visualization To directly compare generated and target sequences, we follow the approach in (Yuan & Qiao, 2024), mapping both into an embedding space using PCA (Shlens, 2014) and t-SNE (Van der Maaten & Hinton, 2008). As shown in Figure 8, the KDE for FLOWTS aligns more closely with the target sequences, especially on the right slope, where Diffusion-TS exhibits noticeable fluctuations, further validating FLOWTS’s superior accuracy.

5. Conclusion

In this work, we address the critical computational inefficiency of diffusion-based time series generation by proposing FLOWTS, an ODE-based model that replaces iterative ODE/SDE solvers with straight-line transport in probabil-

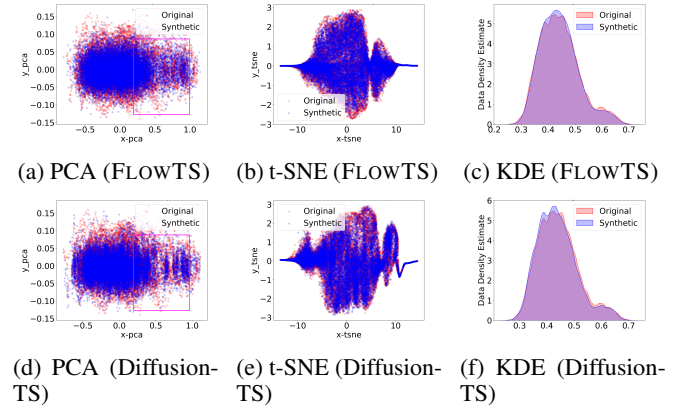


Figure 8: Embedding visualization comparison of generated sequences by FLOWTS and Diffusion-TS methods relative to the target sequences using PCA, t-SNE, and Kernel Density Estimation. Here red indicates the target sequences, where blue indicates the generated sequences.

ity space. By leveraging rectified flow and geodesic paths between two distributions, FLOWTS achieves theoretical optimality while eliminating the need for costly iterative steps, significantly accelerating both training and inference. Our adaptive sampling strategy further enhances efficiency by dynamically balancing noise adaptation and precision.

To ensure high-quality generation, FLOWTS integrates explicit trend and seasonality decomposition, attention registers for global context aggregation, and Rotary Position Embedding (RoPE) to encode positional dependencies. These components collectively address local and global temporal dynamics, enabling authentic and coherent time series synthesis. Extensive experiments validate FLOWTS’s superiority, achieving state-of-the-art FID scores of 0.019 (Stock) and 0.011 (ETTh) and reducing solar forecasting MSE by 43.2% compared to prior methods.

References

- Agarwal, A., Kakade, S. M., Lee, J. D., and Mahajan, G. On the theory of policy gradient methods: Optimality, approximation, and distribution shift. *Journal of Machine Learning Research*, 22(1):1–76, 2021.
- Alcaraz, J. L. and Strodthoff, N. Diffusion-based time series imputation and forecasting with structured state space models. *Transactions on Machine Learning Research*, 2022a. ISSN 2835-8856. URL <https://openreview.net/forum?id=hHiIbk7ApW>.
- Alcaraz, J. M. L. and Strodthoff, N. Diffusion-based time series imputation and forecasting with structured state space models. *arXiv preprint arXiv:2208.09399*, 2022b.
- Campbell, A., Yim, J., Barzilay, R., Rainforth, T., and Jaakkola, T. Generative flows on discrete state-spaces: Enabling multimodal flows with applications to protein co-design. *arXiv preprint arXiv:2402.04997*, 2024.
- Chen, R. T., Rubanova, Y., Bettencourt, J., and Duvenaud, D. K. Neural ordinary differential equations. *Advances in neural information processing systems*, 31, 2018.
- Darcet, T., Oquab, M., Mairal, J., and Bojanowski, P. Vision transformers need registers. *arXiv preprint arXiv:2309.16588*, 2023.
- Desai, A., Freeman, C., Wang, Z., and Beaver, I. Timevae: A variational auto-encoder for multivariate time series generation, 2021. URL <https://arxiv.org/abs/2111.08095>.
- Esser, P., Kulal, S., Blattmann, A., Entezari, R., Müller, J., Saini, H., Levi, Y., Lorenz, D., Sauer, A., Boesel, F., Podell, D., Dockhorn, T., English, Z., Lacey, K., Goodwin, A., Marek, Y., and Rombach, R. Scaling rectified flow transformers for high-resolution image synthesis, 2024. URL <https://arxiv.org/abs/2403.03206>.
- Goodfellow, I., Pouget-Abadie, J., Mirza, M., Xu, B., Warde-Farley, D., Ozair, S., Courville, A., and Bengio, Y. Generative adversarial nets. *Advances in neural information processing systems*, 27, 2014.
- Ho, J., Jain, A., and Abbeel, P. Denoising diffusion probabilistic models. *arXiv preprint arxiv:2006.11239*, 2020.
- Hu, V. T., Yin, W., Ma, P., Chen, Y., Fernando, B., Asano, Y. M., Gavves, E., Mettes, P., Ommer, B., and Snoek, C. G. Motion flow matching for human motion synthesis and editing. *arXiv preprint arXiv:2312.08895*, 2023.
- Jeha, P., Bohlke-Schneider, M., Mercado, P., Kapoor, S., Nirwan, R. S., Flunkert, V., Gasthaus, J., and Januschowski, T. Psa-gan: Progressive self attention gans for synthetic time series. In *The Tenth International Conference on Learning Representations*, 2022.
- Jin, C., Allen-Zhu, Z., Bubeck, S., and Jordan, M. I. Is q-learning provably efficient? *Advances in Neural Information Processing Systems (NeurIPS)*, 31, 2018.
- Jing, B., Berger, B., and Jaakkola, T. Alphafold meets flow matching for generating protein ensembles. *arXiv preprint arXiv:2402.04845*, 2024.
- Karras, T., Aittala, M., Aila, T., and Laine, S. Elucidating the design space of diffusion-based generative models. *Advances in neural information processing systems*, 35: 26565–26577, 2022.
- Kollovieh, M., Ansari, A. F., Bohlke-Schneider, M., Zschiegner, J., Wang, H., and Wang, Y. B. Predict, refine, synthesize: Self-guiding diffusion models for probabilistic time series forecasting. *Advances in Neural Information Processing Systems*, 36, 2024.
- Kong, Z., Ping, W., Huang, J., Zhao, K., and Catanzaro, B. Diffwave: A versatile diffusion model for audio synthesis. *arXiv preprint arXiv:2009.09761*, 2020.
- Kong, Z., Ping, W., Huang, J., Zhao, K., and Catanzaro, B. Diffwave: A versatile diffusion model for audio synthesis, 2021. URL <https://arxiv.org/abs/2009.09761>.
- Kuaishou Technology. Klingai. <https://klingai.kuaishou.com/>, 2024. URL <https://klingai.kuaishou.com/>. Accessed: DATE.
- Lattimore, T. and Szepesvári, C. *Bandit algorithms*. Cambridge University Press, 2020.
- Liao, S., Ni, H., Szpruch, L., Wiese, M., Sabate-Vidales, M., and Xiao, B. Conditional sig-wasserstein gans for time series generation. *arXiv preprint arXiv:2006.05421*, 2020.
- Lim, H., Kim, M., Park, S., and Park, N. Regular time-series generation using sgmm, 2023. URL <https://arxiv.org/abs/2301.08518>.
- Lipman, Y., Chen, R. T., Ben-Hamu, H., Nickel, M., and Le, M. Flow matching for generative modeling. *arXiv preprint arXiv:2210.02747*, 2022.
- Liu, X., Gong, C., and Liu, Q. Flow straight and fast: Learning to generate and transfer data with rectified flow. *arXiv preprint arXiv:2209.03003*, 2022.
- Mehta, S., Tu, R., Beskow, J., Székely, É., and Henter, G. E. Matcha-TTS: A fast TTS architecture with conditional flow matching. In *Proc. ICASSP*, 2024.

- Rasul, K., Seward, C., Schuster, I., and Vollgraf, R. Autoregressive denoising diffusion models for multivariate probabilistic time series forecasting. In *International Conference on Machine Learning*, pp. 8857–8868. PMLR, 2021.
- Shen, L. and Kwok, J. Non-autoregressive conditional diffusion models for time series prediction. In *International Conference on Machine Learning*, pp. 31016–31029. PMLR, 2023.
- Shlens, J. A tutorial on principal component analysis, 2014. URL <https://arxiv.org/abs/1404.1100>.
- Song, Y., Sohl-Dickstein, J., Kingma, D. P., Kumar, A., Ermon, S., and Poole, B. Score-based generative modeling through stochastic differential equations. *arXiv preprint arXiv:2011.13456*, 2020.
- Song, Y., Sohl-Dickstein, J., Kingma, D. P., Kumar, A., Ermon, S., and Poole, B. Score-based generative modeling through stochastic differential equations. *International Conference on Learning Representations (ICLR)*, 2021.
- Su, J., Ahmed, M., Lu, Y., Pan, S., Bo, W., and Liu, Y. Roformer: Enhanced transformer with rotary position embedding. *Neurocomputing*, 568:127063, 2024.
- Sutton, R. S. and Barto, A. G. *Reinforcement Learning: An Introduction*. MIT Press, 2018.
- Tamir, E., Laabid, N., Heinonen, M., Garg, V., and Solin, A. Conditional flow matching for time series modelling. In *ICML 2024 Workshop on Structured Probabilistic Inference* {\&} *Generative Modeling*, 2024.
- Tashiro, Y., Song, J., Song, Y., and Ermon, S. Csd: Conditional score-based diffusion models for probabilistic time series imputation. *Advances in Neural Information Processing Systems*, 34:24804–24816, 2021.
- Van der Maaten, L. and Hinton, G. Visualizing data using t-sne. *Journal of machine learning research*, 9(11), 2008.
- Vaswani, A. Attention is all you need. *Advances in Neural Information Processing Systems*, 2017.
- Wu, L., Wang, D., Gong, C., Liu, X., Xiong, Y., Ranjan, R., Krishnamoorthi, R., Chandra, V., and Liu, Q. Fast point cloud generation with straight flows. In *Proceedings of the IEEE/CVF conference on computer vision and pattern recognition*, pp. 9445–9454, 2023.
- Xiao, G., Tian, Y., Chen, B., Han, S., and Lewis, M. Efficient streaming language models with attention sinks. *arXiv*, 2023.
- Xu, T., Wenliang, L. K., Munn, M., and Acciaio, B. Cotgan: Generating sequential data via causal optimal transport, 2020. URL <https://arxiv.org/abs/2006.08571>.
- Yoon, J., Jarrett, D., and Van der Schaar, M. Time-series generative adversarial networks. *Advances in neural information processing systems*, 32, 2019.
- Yuan, X. and Qiao, Y. Diffusion-TS: Interpretable diffusion for general time series generation. In *The Twelfth International Conference on Learning Representations*, 2024. URL <https://openreview.net/forum?id=4h1apFj099>.
- Zhou, H., Zhang, S., Peng, J., Zhang, S., Li, J., Xiong, H., and Zhang, W. Informer: Beyond efficient transformer for long sequence time-series forecasting. In *The Thirty-Fifth AAAI Conference on Artificial Intelligence, AAAI 2021, Virtual Conference*, volume 35, pp. 11106–11115. AAAI Press, 2021.